Title
A role for monoglyceride lipase in 2-arachidonoylglycerol inactivation

Journal
Chemistry and Physics of Lipids, 121(1-2)

ISSN
0009-3084

Authors
Dinh, Thien P
Freund, Támas F
Piomelli, Daniele

Publication Date
2002-12-01

DOI
10.1016/s0009-3084(02)00150-0

ELSEVIER

Chemistry and Physics of Lipids 121 (2002) 149–158

CPL
CHEMISTRY AND PHYSICS OF LIPIDS

www.elsevier.com/locate/chemphyslip

Review

A role for monoglyceride lipase in 2-arachidonoylglycerol inactivation

Thien P. Dinh [a], Támas F. Freund [b], Daniele Piomelli [a,*]

[a] *Department of Pharmacology, University of California, 360 Med Surge II, Irvine, CA 92697-4625, USA*
[b] *Institute for Experimental Medicine, Hungarian Academy of Sciences, Budapest, Hungary*

Received 13 August 2002; accepted 11 September 2002

Abstract

2-Arachidonoylglycerol (2-AG) is a naturally occurring monoglyceride that activates cannabinoid receptors and meets several key requisites of an endogenous cannabinoid substance. It is present in the brain (where its levels are 170-folds higher than those of anandamide), is produced by neurons in an activity- and calcium-dependent manner, and is rapidly eliminated. The mechanism of 2-AG inactivation is not completely understood, but is thought to involve carrier-mediated transport into cells followed by enzymatic hydrolysis. We examined the possible role of the serine hydrolase, monoglyceride lipase (MGL), in brain 2-AG inactivation. We identified by homology screening a cDNA sequence encoding for a 303-amino acid protein, which conferred MGL activity upon transfection to COS-7 cells. Northern blot and in situ hybridization analyses revealed that MGL mRNA is unevenly present in the rat brain, with highest levels in regions where CB1 cannabinoid receptors are also expressed (hippocampus, cortex, anterior thalamus and cerebellum). Immunohistochemical studies in the hippocampus showed that MGL distribution has striking laminar specificity, suggesting a presynaptic localization of the enzyme. Adenovirus-mediated transfer of MGL cDNA into rat cortical neurons increased the degradation of endogenously produced 2-AG in these cells, whereas no such effect was observed on anandamide degradation. These results indicate that hydrolysis via MGL may be a primary route of 2-AG inactivation in intact neuronal cells.

Keywords: Monoglyceride lipase; 2-Arachidonoylglycerol; Fatty acid amide hydrolase; Anandamide; Endocannabinoids

1. Introduction

The life cycles of the endocannabinoids 2-arachidonoylglycerol (2-AG) and anandamide are similar in that they are both produced by neurons when need arises, act near their site of synthesis, and are rapidly eliminated to terminate their biological actions (Di Marzo et al., 1994; Stella et al., 1997; Piomelli et al., 1999; Beltramo

Abbreviations: 2-AG, 2-arachidonoylglycerol; FAAH, fatty acid amide hydrolase; MGL, monoglyceride lipase; NMDA, *N*-methyl-D-aspartate.

* Corresponding author. Tel.: +1-949-824-6180; fax: +1-949-824-6305
E-mail address: piomelli@uci.edu (D. Piomelli).

0009-3084/02/$ - see front matter © 2002 Published by Elsevier Science Ireland Ltd.
PII: S0009-3084(02)00150-0

and Piomelli, 2000). These properties, which distinguish 2-AG and anandamide from classical or peptide neurotransmitters, reflect the suggested role of these bioactive lipids as activity-dependent, short-range modulators of synaptic function. Neurochemical and electrophysiological data directly support such a role. For example, microdialysis experiments in the rat striatum indicate that locally released anandamide may serve as a negative feedback signal regulating dopaminergic activity (Giuffrida et al., 1999; Beltramo et al., 2000). In addition, electrophysiological experiments suggest that anandamide or 2-AG may act as transsynaptic messengers to modulate neurotransmitter release (Katona et al., 1999; Kreitzer and Regehr, 2001; Ohno-Shosaku et al., 2001; Wilson and Nicoll, 2001) and synaptic plasticity (Carlson et al., 2002; Gerdeman et al., 2002; Marsicano et al., 2002; Robbe et al., 2002) in neurons.

Despite these broad analogies, the specific routes by which 2-AG and anandamide are produced and inactivated appear to be quite different. Anandamide is thought to be generated from the hydrolysis of an *N*-acylated species of phosphatidylethanolamine (PE), *N*-arachidonoyl-PE, which requires the activity of an unknown phospholipase D (Di Marzo et al., 1994; Cadas et al., 1996; Sugiura et al., 1996; Cadas et al., 1997). By contrast, 2-AG synthesis may involve the same enzymatic cascade that catalyzes the formation of the second messengers inositol-(1,4,5)-trisphosphate and 1,2-diacylglycerol (DAG). Phospholipase C (PLC) acting on membrane phosphoinositides generates DAG, which is then converted to 2-AG by a DAG-lipase activity (Stella et al., 1997).

After release, anandamide may be accumulated back into neurons and glial cells by means of an energy- and Na^+-independent transport system (Di Marzo et al., 1994; Beltramo et al., 1997), and may be broken down intracellularly to arachidonic acid and ethanolamine by fatty acid amide hydrolase (FAAH) or other amidase enzymes (Schmid et al., 1985; Cravatt et al., 1996; Ueda et al., 2001). There is evidence suggesting that 2-AG may be transported into cells through a mechanism similar to that of anandamide. For example, in human astrocytoma and other cell types, [^{3}H]anandamide and [^{3}H]2-AG transport have similar kinetic properties (Piomelli et al., 1999; Bisogno et al., 2001). Moreover, anandamide and 2-AG can prevent each other's transport (Beltramo and Piomelli, 2000; Bisogno et al., 2001). Finally, the accumulation of both endocannabinoids is blocked by the anandamide analog 4-(hydroxyphenyl)-arachidonamide (AM404) (Beltramo and Piomelli, 2000; Bisogno et al., 2001). Yet, significant differences between anandamide and 2-AG transport also have been documented. [^{3}H]2-AG uptake by astrocytoma cells is inhibited by arachidonic acid, whereas [^{3}H]anandamide accumulation is not (Beltramo and Piomelli, 2000). This discrepancy may be explained in two alternative ways. Arachidonic acid may directly interfere with a 2-AG carrier distinct from anandamide's; or the fatty acid may indirectly prevent the facilitated diffusion of 2-AG by inhibiting its enzymatic conversion to arachidonic acid. If the latter explanation is correct, agents that interfere with the incorporation of arachidonic acid into phospholipids, such as triacsin C (an inhibitor of acyl–coenzyme A synthesis), also should decrease [^{3}H]2-AG uptake. This is indeed the case in astrocytoma cells (Beltramo and Piomelli, 2000). Thus, while anandamide and 2-AG may be internalized through similar transport mechanisms, or even share a common one, they appear to differ in how their intracellular breakdown can affect the rate of transport into cells.

The fact that FAAH catalyzes the hydrolysis of both 2-AG and anandamide in vitro has led to the suggestion that this enzyme may be responsible for the elimination of both endocannabinoids. This hypothesis is contradicted, however, by several observations. Synthetic 2-AG is rapidly degraded in mouse blood whereas anandamide is stable under the same conditions (Jarai et al., 2000). In addition, inhibitors of FAAH activity have no effect on 2-AG hydrolysis at concentrations that completely block anandamide degradation (Beltramo and Piomelli, 2000). Furthermore, 2-AG hydrolysis is preserved in mutant $FAAH^{-/-}$ mice, which cannot dispose of either endogenous or exogenous anandamide (Lichtman et al., 2002). In agreement with these results, a 2-AG-hydrolase

activity distinct from FAAH has been partially purified from porcine brain (Goparaju et al., 1999b). This activity may correspond to monoacylglycerol lipase (MGL), a cytosolic serine hydrolase that converts 2- and 1-monoglycerides to fatty acid and glycerol (Karlsson et al., 1997). To test this hypothesis, we have cloned and characterized rat brain MGL (Dinh et al., 2002).

2. Results

2.1. Cloning of rat brain MGL

We used a 1 kilobase (kb) fragment of mouse adipocyte MGL cDNA to screen a rat brain cDNA library by low-stringency hybridization. Upon initial screening of 2.5×10^5 phage plaques, we identified 40 positive clones, which we purified and subjected to secondary and tertiary screenings to ensure homogeneity. After phage purification, we transformed plasmids into competent bacteria and conducted restriction analysis to identify positive clones. We selected for sequencing five random inserts that were greater than 1 kb in size. The inserts overlapped and together represented the entire open reading frame of MGL.

The nucleotide and predicted amino acid sequence of rat brain MGL are depicted in Fig. 1. Based on the deduced amino acid sequence, rat brain MGL comprises 303 amino acids with a calculated molecular weight of 33 367 Da. Alignment between rat brain and mouse adipocyte MGL revealed that the two nucleotide sequences are 92% identical. The residues composing the catalytic triad are conserved, as are the GSXSG and HG dipeptide motifs commonly found in lipases (Karlsson et al., 1997). Consistent with this homology, transient expression in COS-7 cells showed that rat MGL cDNA encodes for a functionally active enzyme (Fig. 2). Primary sequence analysis of rat MGL did not reveal any homology with FAAH or any member of the 'amidase signature' family of enzymes. Furthermore, the analysis did not identify any obvious post-translational motif in MGL, though it did disclose several consensus sequences for phosphorylation by protein kinases, including Ca^{2+}/calmodulin kinase II and protein kinases A and C.

```
ATGCCTGAGGCAAGTTCACCCAGGCGAACTCCACAGAACGTCCCCTACCAGGACCTTCCT    60
M  P  E  A  S  S  P  R  R  T  P  Q  N  V  P  Y  Q  D  L  P      20

CACCTGGTCAATGCGGATGGACAGTACCTCTTTTGTAGGTACTGGAAGCCCAGTGGCACA   120
H  L  V  N  A  D  G  Q  Y  L  F  C  R  Y  W  K  P  S  G  T      40

CCCAAGGCCCTCATCTTCGTGTCCCATGGAGCTGGGGAACACTGTGGCCGTTATGACGAG   180
P  K  A  L  I  F  V  S  H  G  A  G  E  H  C  G  R  Y  D  E      60

CTGGCTCAGATGTTGAAGAGGCTGGACATGCTGGTGTTTGCCCATGACCATGTTGGCCAT   240
L  A  Q  M  L  K  R  L  D  M  L  V  F  A  H  D  H  V  G  H      80

GGGCAGAGCGAGGGAGAGAGGATGGTGGTATCGGACTTCCAAGTTTTTGTCAGAGATTTG   300
G  Q  S  E  G  E  R  M  V  V  S  D  F  Q  V  F  V  R  D  L     100

TTGCAGCACGTGAACACCGTCCAGAAGGACTACCCCGAGGTCCCCGTCTTCCTCCTGGGC   360
L  Q  H  V  N  T  V  Q  K  D  Y  P  E  V  P  V  F  L  L  G     120

CACTCCATGGGCGGTGCCATCTCCATCCTAGCAGCTGCAGAGAGACCAACCCACTTTTCT   420
H  S  M  G  G  A  I  S  I  L  A  A  A  E  R  P  T  H  F  S     140

GGCATGATCCTAATTTCACCTCTGATCCTTGCCAATCCGGAATCTGCATCGACTTTGAAG   480
G  M  I  L  I  S  P  L  I  L  A  N  P  E  S  A  S  T  L  K     160

GTCCTTGCTGCCAAACTGCTCAATTTTGTCCTGCCAAACATATCCTTGGGGCGCATCGAC   540
V  L  A  A  K  L  L  N  F  V  L  P  N  I  S  L  G  R  I  D     180

TCCAGCGTGCTGTCTCGGAACAAGTCGGAGGTTGACCTGTACAACTCCGACCCACTCATC   600
S  S  V  L  S  R  N  K  S  E  V  D  L  Y  N  S  D  P  L  I     200

TGCCACGCAGGGGTGAAGGTATGCTTTGGCATCCAGCTGCTGAACGCTGTCTCGAGGGTG   660
C  H  A  G  V  K  V  C  F  G  I  Q  L  L  N  A  V  S  R  V     220

GAGCGAGCAATGCCCAGGCTGACACTGCCGTTCCTGCTGCTGCAGGGTTCTGCTGACCGG   720
E  R  A  M  P  R  L  T  L  P  F  L  L  L  Q  G  S  A  D  R     240

CTTTGCGACAGCAAAGGTGCCTACCTGCTCATGGAATCATCCCCGAGTCAGGACAAAACA   780
L  C  D  S  K  G  A  Y  L  L  M  E  S  S  P  S  Q  D  K  T     260

CTCAAGATGTATGAAGGTGCCTACCATGTTCTCCACAAGGAGCTTCCGGAAGTGACCAAC   840
L  K  M  Y  E  G  A  Y  H  V  L  H  K  E  L  P  E  V  T  N     280

TCTGTCCTCCATGAAATAAATACGTGGGTGTCTCACAGGATAGCAGTGGCAGGAGCTAGG   900
S  V  L  H  E  I  N  T  W  V  S  H  R  I  A  V  A  G  A  R     300

TGTCTACCCTGA                                                   912
C  L  P  *                                                     303
```

Fig. 1. Nucleotide and deduced amino acid sequence of rat brain MGL cDNA. Closed circles mark amino acid residues comprising the putative catalytic triad. The HG dipeptide motif often found in lipases is boxed.

Northern blot analyses of total RNA from various regions of the rat brain showed a single transcript of $\approx$4 kb, a size that corresponds to that of mouse MGL (Karlsson et al., 1997; Fig. 3a). MGL mRNA was present throughout the brain, but its expression varied among regions, with high levels in cerebellum, cortex and hippocampus; intermediate levels in thalamus and striatum; and lower levels in brainstem and hypothalamus (Fig. 3a). Densitometric measurements of representative Northern blots provided the following average optical density values (in arbitrary units): cortex, 7.5; hippocampus, 6.8; cerebellum, 6.1; thalamus, 5.4; striatum, 4.6; hypothalamus, 1.2; brainstem, 1.0. Western blot analyses confirmed the presence of MGL protein in brain tissue. Using an immunopurified poly-

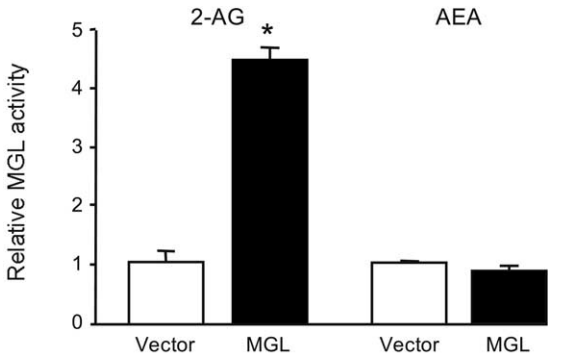

Fig. 2. Heterologous expression of MGL in COS-7 cells. Five μg of MGL cDNA was transfected into COS-7 cells by calcium phosphate precipitation. 48 h post-transfection cells were harvested, lysed and centrifuged. The supernatant fraction (50 μg protein) was incubated in 50 mM sodium phosphate (pH 8.0) with either [^{3}H]2-AG or [^{3}H]anandamide (5000 cpm for both). MGL activity in vector-transfected (open bars) and MGL-transfected (closed bars) cells; results are from three experiments performed in triplicate. *, $P < 0.05$, Student's t-test.

clonal antibody to the N-terminal sequence of rat MGL, we observed two protein bands migrating at ~35 and ~37 kDa on SDS-polyacrylamide gels (Fig. 3b). Both bands were abolished by adsorption with the immunizing peptide (data not shown), an indication that they represent closely related MGL isoforms. These could arise from either alternative splicing (Karlsson et al., 2001) or as-yet-unidentified post-translational modification(s).

2.2. Brain localization of MGL

As MGL is generally thought to serve 'housekeeping' functions in lipid metabolism, we were surprised by the uneven distribution of MGL expression revealed by our Northern blot analyses (Fig. 3). We set out, therefore, to investigate in greater detail the brain distribution of MGL by using two complementary approaches: in situ hybridization and immunohistochemistry.

In situ hybridization analyses showed that MGL mRNA is highly expressed throughout the rat brain cortex, with the transcript mainly concentrated in layers IV, deep V and VI (Fig. 4a–c), in the hippocampus, where it was abundant in the CA3 field (Fig. 3c and e), and in the cerebellum (Fig. 4b). MGL mRNA expression was also remarkably high in the anterior thalamus, particularly in the anterodorsal nucleus (Fig. 4b), but not in other thalamic areas (Fig. 4b and c). Moderate amounts of MGL mRNA were detected in the nucleus accumbens shell (Fig. 4a), in the islands of Calleja and in the pontine nuclei (data not shown). We observed no specific signal in tissue sections hybridized with a sense probe (Fig. 4d).

We conducted light microscopic immunostaining studies in the rat hippocampus with the immunopurified polyclonal antibody used for our Western blot analyses (Fig. 3b). These studies show a distinct laminar pattern of MGL staining in the hippocampus and a profound difference in staining intensity between the stratum radiatum

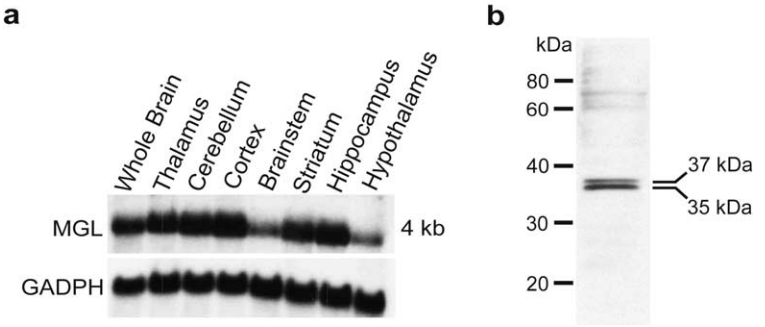

Fig. 3. MGL is expressed in the rat brain. (A) Representative Northern blot of MGL mRNA from various regions of the rat brain; glyceraldehyde-3-phosphate-dehydrogenase (GADPH) mRNA was used as a loading control. (B) Representative Western blot of supernatant fraction from the rat brain.

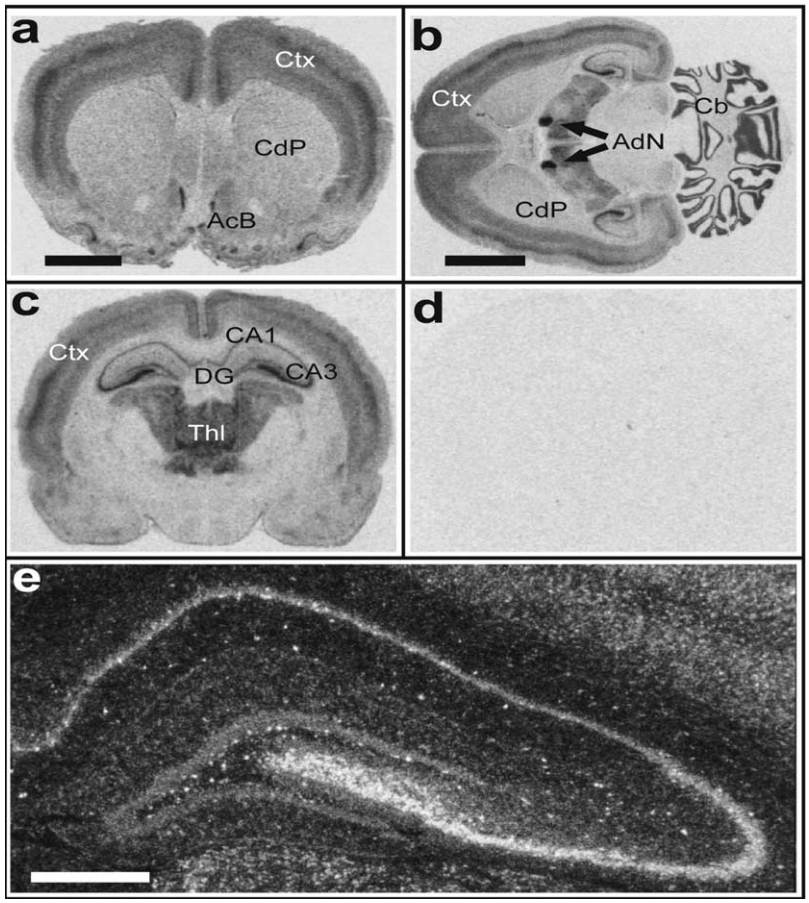

Fig. 4. Distribution of MGL mRNA in the rat brain. Coronal (A and C) and horizontal (B) sections hybridized with an MGL antisense riboprobe labeled with [^{35}S]UTP. (D) Horizontal section hybridized with a sense probe. (E) Dark field micrograph of MGL-positive cells in the hippocampus. Abbreviations: AcB, nucleus accumbens; AdN, anterodorsal nucleus of the thalamus; Cb cerebellum; CdP, caudate–putamen; Ctx, cortex; DG, dentate gyrus; Thl, thalamus. Scales: A, 3 mm; B, 4 mm; E, 500 μm.

(where glutamatergic terminals from hippocampal CA3 pyramidal neurons terminate) and the stratum lacunosum-moleculare (where glutamatergic terminals from the entorhinal cortex terminate) (Fig. 5a and b). In the stratum pyramidale, the somata of pyramidal cells were not stained by the MGL antibody, but were surrounded by MGL-positive terminals of γ-aminobutyric acid (GABA)-ergic interneurons (basket cell) (Fig. 5c). In the CA3 field, the glutamatergic mossy fiber terminals in stratum lucidum were strongly stained and clearly discernible within the MGL-positive background (Fig. 5c). Mossy fiber collaterals and GABA-ergic basket cell axons surrounded somata and proximal dendrites also in the hilus of the dentate gyrus. Granule cell bodies were MGL-negative and surrounded by positive basket axons. In sections prepared by osmium treatment, the immuno-negative apical dendrites of pyramidal cells could be readily traced through the densely stained neuropil of stratum radiatum, indicating that this neuropil staining derived mostly, if not entirely, from MGL localized in axon terminals (Fig. 5d). Control sections in which the antibody was pre-adsorbed with the immunizing peptide showed no specific staining (data not shown).

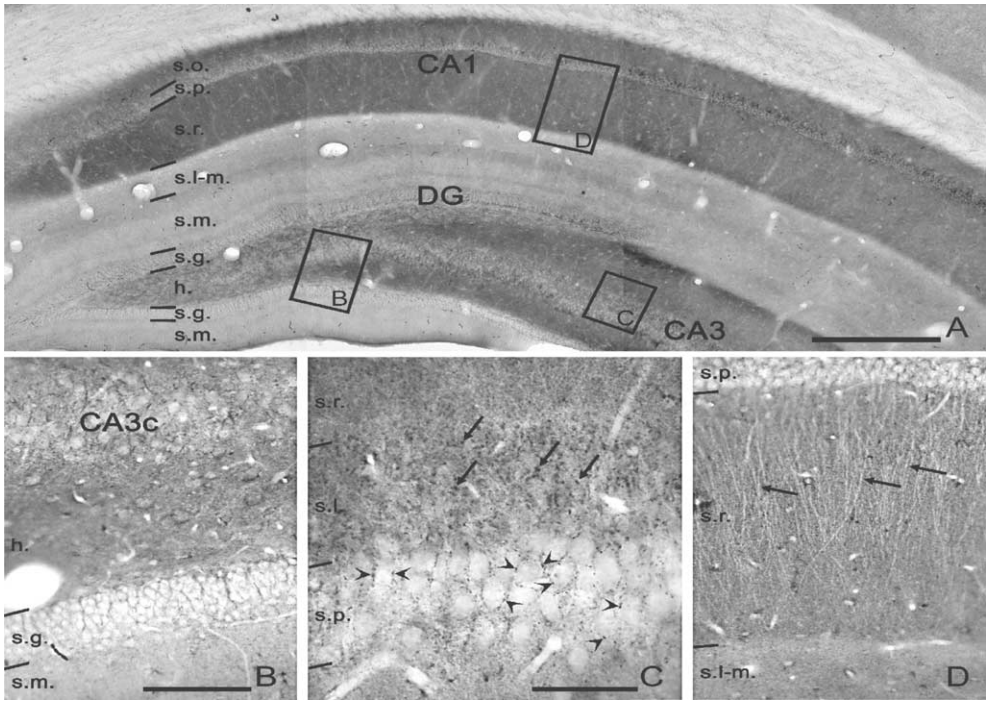

Fig. 5. Distribution of MGL protein in the rat brain. (A) Light micrograph of a hippocampal section immunostained for MGL. At higher magnification (B–D), cell bodies of principal cells in all subfields are not stained by the antibody, but are surrounded by MGL-positive axon terminals (arrowheads in C), which may represent boutons of GABA-ergic interneurons (basket cells). Mossy fiber terminals in CA3 stratum lucidum (arrows in C) are densely immunostained. (D) Light micrograph of an osmium-treated section from CA1, showing that pyramidal dendrites in stratum radiatum (arrows) appear as negative images in the heavily stained neuropil. Abbreviations: DG, dentate gyrus; h., hilus; s.g., stratum granulosum; s.l., s. lucidum; s.l.m., s. lacunosum-moleculare; s.m., s. moleculare; s.o., s. oriens; s.p., s. pyramidale; s.r., s. radiatum. Scales: A, 500 μm; B–D, 100 μm.

2.3. 2-AG, not anandamide, is a substrate for MGL

Since FAAH hydrolyzes anandamide and 2-AG at comparable rates in vitro (Goparaju et al., 1999a; Patricelli and Cravatt, 1999), we examined whether rat brain MGL also utilizes anandamide and other fatty acid ethanolamides as substrates. To this aim, we generated an adenoviral vector containing MGL cDNA to allow for the over-expression of MGL in neurons and other mammalian cells.

Infection with MGL-bearing adenovirus conferred high levels of MGL immunoreactivity to HeLa cells (Fig. 6a), which normally do not express this protein (Fig. 6b). The immunoreactivity was associated with both cell cytosol and plasma membranes (Fig. 6a). MGL activity was also markedly elevated in MGL-infected HeLa cells (Fig. 6c) and was similarly distributed between cytosol and membranes: after ultracentrifugation, MGL activity was recovered both in supernatant and particulate fractions (in pmol/min per mg protein; supernatant: 0.28; particulate, 0.14; $n = 3$).

Various serine hydrolase inhibitors that were previously shown to block FAAH also inhibited MGL activity, including methyl arachidonylfluorophosphonate (half-maximal inhibitory concentration, IC_{50}, 0.8 ± 0.05 μM; $n = 3$) and arachidonyl trifluoromethylketone (IC_{50}, 2.5 ± 0.04 μM) (Fig. 7a). Interestingly, hexadecylsulphonylfluoride (AM374), which is potent at inhibiting FAAH activity (IC_{50} for FAAH, 10.2 ± 0.1 nM), only weakly inhibited MGL activity (IC_{50} for MGL,

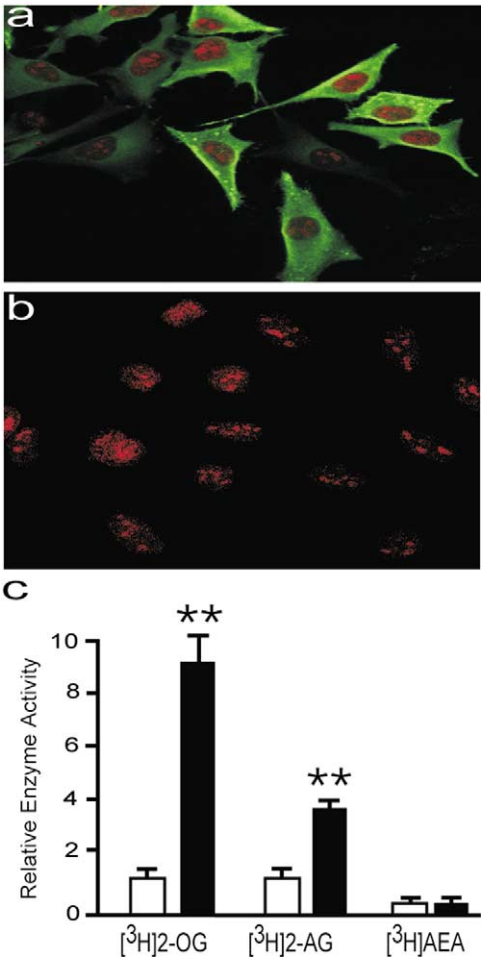

Fig. 6. MGL overexpression in HeLa cells. Confocal microscopy images of cells infected with MGL-bearing (A) or control (B) adenovirus. MGL immunoreactivity is shown in green; cell nuclei in red. (C) MGL activity in vector- (open bars) or MGL-infected (closed bar) cells. [^{3}H]2-OG, 2-oleoyl-[^{3}H]glycerol; [^{3}H]AEA, [^{3}H]anandamide. Results are expressed as the mean ± S.E.M. of three experiments performed in triplicate. **, $P < 0.01$, Student's t-test.

6.2 ± 0.1 μM) (Fig. 7b). MGL hydrolyzed 2-[^{3}H]AG and 2-[^{3}H]oleoylglycerol, not [^{3}H]anandamide, [^{3}H]palmitoylethanolamide or [^{3}H]oleoylethanolamide (Fig. 6 and data not shown), indicating that the enzyme preferentially recognizes 2-monoglycerides over fatty acid ethanolamides.

2.4. MGL degrades endogenously produced 2-AG in intact neurons

Previous work has shown that the concomitant activation of glutamate NMDA-type receptors and cholinergic receptors stimulates the production of both 2-AG and anandamide in rat cortical neurons (Stella and Piomelli, 2001). We reasoned that if MGL selectively mediates 2-AG inactivation, changes in this enzyme activity should affect 2-AG accumulation while leaving anandamide's unchanged. To test this prediction, we overexpressed MGL in neurons by means of adenoviral transfer. Compared with vector-infected neurons (Fig. 8a and b), neurons infected with MGL-containing adenovirus expressed substantially larger amounts of MGL mRNA (Fig. 8a) and protein (Fig. 8b). As expected, the main transcript in MGL-overexpressing neurons corresponded to the 1.2 kb coding sequence of MGL (Fig. 8a).

In control neurons labeled by incubation with [^{3}H]arachidonic acid, co-activation of *N*-methyl-D-aspartate (NMDA) and cholinergic receptors with a combination of NMDA and carbachol produced a rapid increase in [^{3}H]2-AG levels (Fig. 8d), which was significantly reduced in MGL-overexpressing neurons (Fig. 8d). Control experiments indicated that this reduction likely reflects increased 2-AG breakdown, rather than decreased 2-AG synthesis. Formation of 2-AG occurs via enzymatic hydrolysis of DAG, which is generated through Ca^{2+}-dependent cleavage of phosphoinositides by PLC (Stella et al., 1997). Neither of these reactions was affected by MGL overexpression: vector- and MGL-infected neurons had equivalent levels of stimulated DAG production (in cpm per dish; vector: 6700 ± 385; MGL: 6370 ± 440; $n = 8$) and $[Ca^{2+}]_i$ rises (assessed by Fura-2 imaging; data not shown). Thus, MGL overexpression may enhance 2-AG inactivation without changing receptor-dependent 2-AG formation. Is this enhancement selective for 2-AG? To answer this question, we concurrently quantified 2-AG and anandamide by using an isotope-dilution HPLC/MS method. In vector-infected neurons, the levels of both endocannabinoids significantly increased after a 2.5 min stimulation with NMDA/carbachol (Fig. 8e). By contrast, in

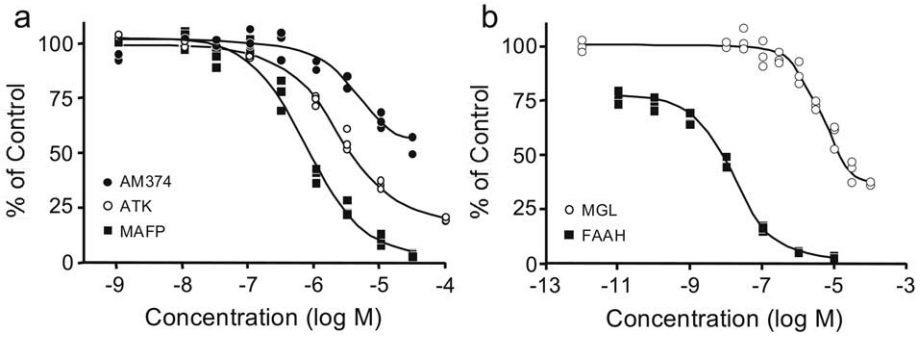

Fig. 7. Pharmacological inhibition of MGL and FAAH activity by serine hydrolase inhibitors. (a) MGL activity inhibition in MGL-overexpressing HeLa cells by arachidonyltrifluoromethylketone (ATMK), methyl arachidonylfluorophosphonate (MAFP) and hexadecylsulphonylfluoride (AM374). (b) Inhibition of rat brain MGL and FAAH activities by AM374.

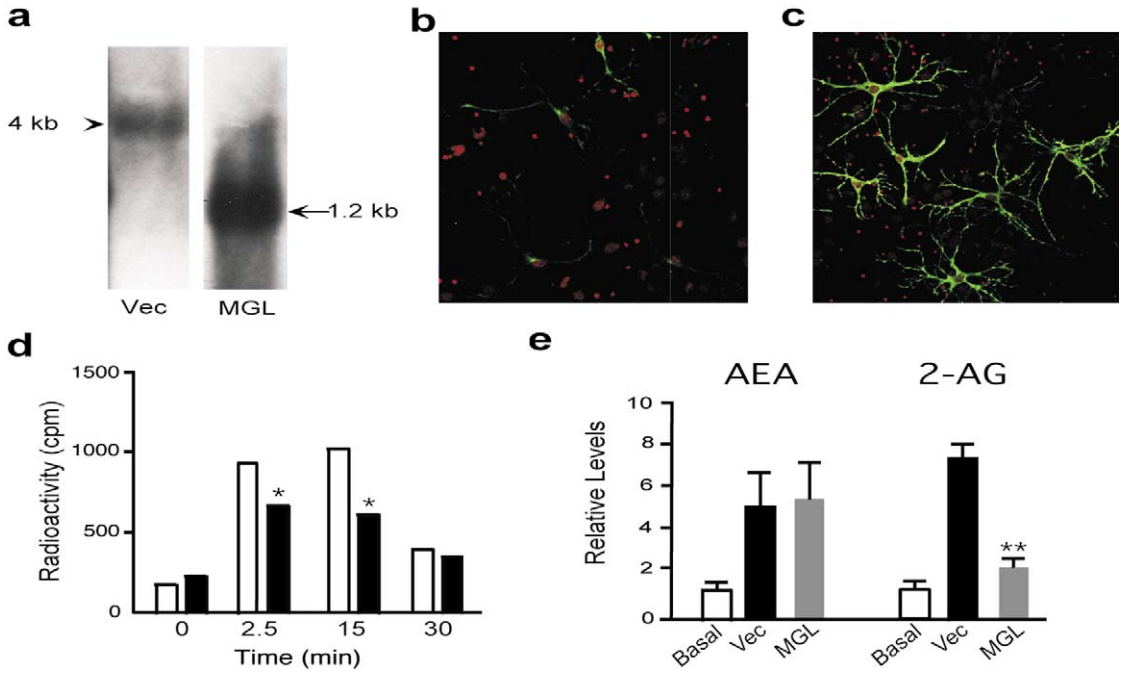

Fig. 8. MGL overexpression curtails receptor-dependent 2-AG accumulation in rat cortical neurons. Expression of MGL mRNA (A) and protein (B) in vector- and MGL-infected neurons. Confocal microscopy images of vector- (B) and MGL-infected (C) neurons. Vector-infected cells contain low, but detectable levels of endogenous MGL. MGL immunoreactivity is shown in green; cell nuclei in red. (D) Time course of [^{3}H]2-AG accumulation following concomitant stimulation of NMDA and cholinergic receptors in vector- (open bars) and MGL-infected (filled bars) neurons. Results are from one experiment, representative of four. (E) HPLC/MS quantification of 2-AG and anandamide accumulation in neurons. Open bars, unstimulated vector-infected neurons; filled bars, stimulated vector-infected neurons; shaded bars, stimulated MGL-infected neurons. Left panel, anandamide (AEA) levels; right panel,

MGL-overexpressing cells, 2-AG accumulation was greatly reduced after the stimulation, whereas anandamide levels increased to the same extent as they did in vector-infected neurons (Fig. 8e).

3. Discussion

Two findings of this study are relevant to a role of MGL in 2-AG inactivation. The first is that

adenovirus-mediated overexpression of MGL in cortical neurons attenuated the receptor-dependent accumulation of endogenous 2-AG, but had no effect on either 2-AG synthesis or anandamide hydrolysis. A plausible interpretation of these results is that hydrolysis by means of MGL may be a primary route of 2-AG elimination in intact neurons. The second finding is that, unlike FAAH (Thomas et al., 1997; Tsou et al., 1998b; Romero et al., 2002), MGL was discretely distributed throughout the central nervous system. We observed high levels of MGL mRNA in relatively few areas of the brain, which include the hippocampus, cerebellum, anterodorsal nucleus of the thalamus and the cortex. These brain regions also contain CB1 cannabinoid receptors (Herkenham et al., 1991; Tsou et al., 1998a), supporting a function for MGL in terminating the effects of 2-AG at these receptors.

What are the physiological roles of MGL, if any, and what interest may this enzyme have as a target for therapeutic drugs? This question can be adequately answered only with the development of selective MGL inhibitors and the generation of mutant mice lacking a functional MGL gene. But our findings may shed some light on at least one possible role of MGL. In the hippocampus, electrical stimulation of the Schaffer collaterals, a glutamatergic fiber tract that projects from CA3 to CA1 neurons, enhances 2-AG synthesis (Stella et al., 1997). Newly generated 2-AG may in turn inhibit GABA release, via CB1 receptors on basket cell terminals (Wilson and Nicoll, 2001), and glutamate release, via as-yet-unidentified CB1-like receptors on Schaffer terminals (Hajos et al., 2001). Our results, showing that MGL is highly expressed in the termination zones of Schaffer collaterals, suggest a presynaptic localization of this enzyme and provide an anatomical locus for 2-AG deactivation at hippocampal synapses.

Acknowledgements

We thank Dr C. Holm for the generous gift of mouse adipocyte MGL cDNA; Dr F.M. Leslie and Dr D. Carpenter for help with experiments; Dr M.-L. Solbrig and Dr A. Giuffrida for critical reading of the manuscript; Dr C. Gall for discussion. This work was supported by the National Institute on Drug Abuse Grants 12447 and 3412 (to D. Piomelli) and by the Howard Hughes Medical Institute and OTKA (to T.F. Freund). T.P. Dinh was supported by National Institute of Aging fellowship AG00096.

References

Beltramo, M., Piomelli, D., 2000. Carrier-mediated transport and enzymatic hydrolysis of the endogenous cannabinoid 2-arachidonylglycerol. Neuroreport 11, 1231–1235.

Beltramo, M., Stella, N., Calignano, A., Lin, S.Y., Makriyannis, A., Piomelli, D., 1997. Functional role of high-affinity anandamide transport, as revealed by selective inhibition. Science 277, 1094–1097.

Beltramo, M., Rodríguez de Fonseca, F., Navarro, M., Calignano, A., Gorriti, M.A., Grammatikopoulos, G., Sadile, A.G., Giuffrida, A., Piomelli, D., 2000. Reversal of dopamine D_2 receptor responses by an anandamide transport inhibitor. J. Neurosci. 20, 3401–3407.

Bisogno, T., MacCarrone, M., De Petrocellis, L., Jarrahian, A., Finazzi-Agro, A., Hillard, C., Di Marzo, V., 2001. The uptake by cells of 2-arachidonoylglycerol, an endogenous agonist of cannabinoid receptors. Eur. J. Biochem. 268, 1982–1989.

Cadas, H., Gaillet, S., Beltramo, M., Venance, L., Piomelli, D., 1996. Biosynthesis of an endogenous cannabinoid precursor in neurons and its control by calcium and cAMP. J. Neurosci. 16, 3934–3942.

Cadas, H., di Tomaso, E., Piomelli, D., 1997. Occurrence and biosynthesis of endogenous cannabinoid precursor, *N*-arachidonoyl phosphatidylethanolamine, in rat brain. J. Neurosci. 17, 1226–1242.

Carlson, G., Wang, Y., Alger, B.E., 2002. Endocannabinoids facilitate the induction of LTP in the hippocampus. Nat. Neurosci. 5, 723–724.

Cravatt, B.F., Giang, D.K., Mayfield, S.P., Boger, D.L., Lerner, R.A., Gilula, N.B., 1996. Molecular characterization of an enzyme that degrades neuromodulatory fatty-acid amides. Nature 384, 83–87.

Di Marzo, V., Fontana, A., Cadas, H., Schinelli, S., Cimino, G., Schwartz, J.C., Piomelli, D., 1994. Formation and inactivation of endogenous cannabinoid anandamide in central neurons. Nature 372, 686–691.

Dinh, T.P., Carpenter, D., Leslie, F.M., Freund, T.F., Katona, I., Sensi, S.L., Kathuria, S., Piomelli, D., 2002. Brain monoglyceride lipase participating in endocannabinoid inactivation. Proc. Natl. Acad. Sci. USA 99, 10819–10824.

Gerdeman, G.L., Ronesi, J., Lovinger, D.M., 2002. Postsynaptic endocannabinoid release is critical to long-term depression in the striatum. Nat. Neurosci. 5, 446–451.

Giuffrida, A., Parsons, L.H., Kerr, T.M., Rodríguez de Fonseca, F., Navarro, M., Piomelli, D., 1999. Dopamine activation of endogenous cannabinoid signaling in dorsal striatum. Nat. Neurosci. 2, 358–363.

Goparaju, S.K., Kurahashi, Y., Suzuki, H., Ueda, N., Yamamoto, S., 1999a. Anandamide amidohydrolase of porcine brain: cDNA cloning, functional expression and site-directed mutagenesis(1). Biochim. Biophys. Acta 1441, 77–84.

Goparaju, S.K., Ueda, N., Taniguchi, K., Yamamoto, S., 1999b. Enzymes of porcine brain hydrolyzing 2-arachidonoylglycerol, an endogenous ligand of cannabinoid receptors. Biochem. Pharmacol. 57, 417–423.

Hajos, N., Ledent, C., Freund, T.F., 2001. Novel cannabinoid-sensitive receptor mediates inhibition of glutamatergic synaptic transmission in the hippocampus. Neuroscience 106, 1–4.

Herkenham, M., Lynn, A.B., Johnson, M.R., Melvin, L.S., de Costa, B.R., Rice, K.C., 1991. Characterization and localization of cannabinoid receptors in rat brain: a quantitative in vitro autoradiographic study. J. Neurosci. 11, 563–583.

Jarai, Z., Wagner, J.A., Goparaju, S.K., Wang, L., Razdan, R.K., Sugiura, T., Zimmer, A.M., Bonner, T.I., Zimmer, A., Kunos, G., 2000. Cardiovascular effects of 2-arachidonoyl glycerol in anesthetized mice. Hypertension 35, 679–684.

Karlsson, M., Contreras, J.A., Hellman, U., Tornqvist, H., Holm, C., 1997. cDNA cloning, tissue distribution, and identification of the catalytic triad of monoglyceride lipase. Evolutionary relationship to esterases, lysophospholipases, and haloperoxidases. J. Biol. Chem. 272, 27218–27223.

Karlsson, M., Reue, K., Xia, Y.R., Lusis, A.J., Langin, D., Tornqvist, H., Holm, C., 2001. Exon–intron organization and chromosomal localization of the mouse monoglyceride lipase gene. Gene 272, 11–18.

Katona, I., Sperlagh, B., Sik, A., Kafalvi, A., Vizi, E.S., Mackie, K., Freund, T.F., 1999. Presynaptically located CB1 cannabinoid receptors regulate GABA release from axon terminals of specific hippocampal interneurons. J. Neurosci. 19, 4544–4558.

Kreitzer, A.C., Regehr, W.G., 2001. Retrograde inhibition of presynaptic calcium influx by endogenous cannabinoids at excitatory synapses onto Purkinje cells. Neuron 29, 717–727.

Lichtman, A.H., Hawkins, E.G., Griffin, G., Cravatt, B.F., 2002. Pharmacological activity of fatty acid amides is regulated, but not mediated, by fatty acid amide hydrolase in vivo. J. Pharmacol. Exp. Ther. 302, 73–79.

Marsicano, G., Wotjak, C.T., Azad, S.C., Bisogno, T., Rammes, G., Cascio, M.G., Hermann, H., Tang, J., Hofmann, C., Zieglgansberger, W., Di Marzo, V., Lutz, B., 2002. The endogenous cannabinoid system controls extinction of aversive memories. Nature 418, 530–534.

Ohno-Shosaku, T., Maejima, T., Kano, M., 2001. Endogenous cannabinoids mediate retrograde signals from depolarized postsynaptic neurons to presynaptic terminals. Neuron 29, 729–738.

Patricelli, M.P., Cravatt, B.F., 1999. Fatty acid amide hydrolase competitively degrades bioactive amides and esters through a nonconventional catalytic mechanism. Biochemistry 38, 14125–14130.

Piomelli, D., Beltramo, M., Glasnapp, S., Lin, S.Y., Goutopoulos, A., Xie, X.Q., Makriyannis, A., 1999. Structural determinants for recognition and translocation by the anandamide transporter. Proc. Natl. Acad. Sci. USA 96, 5802–5807.

Robbe, D., Kopf, M., Remaury, A., Bockaert, J., Manzoni, O.J., 2002. Endogenous cannabinoids mediate long-term synaptic depression in the nucleus accumbens. Proc. Natl. Acad. Sci. USA 99, 8384–8388.

Romero, J., Hillard, C.J., Calero, M., Rábano, A., 2002. Fatty acid amide hydrolase localization in the human central nervous system: an immunohistochemical study. Mol. Brain Res. 100, 85–93.

Schmid, P.C., Zuzarte-Augustin, M.L., Schmid, H.H., 1985. Properties of rat liver *N*-acylethanolamine amidohydrolase. J. Biol. Chem. 260, 14145–14149.

Stella, N., Piomelli, D., 2001. Receptor-dependent formation of endogenous cannabinoids in cortical neurons. Eur. J. Pharmacol. 425, 189–196.

Stella, N., Schweitzer, P., Piomelli, D., 1997. A second endogenous cannabinoid that modulates long-term potentiation. Nature 388, 773–778.

Sugiura, T., Kondo, S., Sukagawa, A., Tonegawa, T., Nakane, S., Yamashita, A., Ishima, Y., Waku, K., 1996. Transacylase-mediated and phosphodiesterase-mediated synthesis of *N*-arachidonoylethanolamine, an endogenous cannabinoid–receptor ligand, in rat brain microsomes. Comparison with synthesis from free arachidonic acid and ethanolamine. Eur. J. Biochem. 240, 53–62.

Thomas, E.A., Cravatt, B.F., Danielson, P.E., Gilula, N.B., Sutcliffe, J.G., 1997. Fatty acid amide hydrolase, the degradative enzyme for anandamide and oleamide, has selective distribution in neurons within the rat central nervous system. J. Neurosci. Res. 50, 1047–1052.

Tsou, K., Brown, S., Sañudo-Peña, M.C., Mackie, K., Walker, J.M., 1998a. Immunohistochemical distribution of cannabinoid CB1 receptors in the rat central nervous system. Neuroscience 83, 393–411.

Tsou, K., Nogueron, M.I., Muthian, S., Sanudo-Pena, M.C., Hillard, C.J., Deutsch, D.G., Walker, J.M., 1998b. Fatty acid amide hydrolase is located preferentially in large neurons in the rat central nervous system as revealed by immunohistochemistry. Neurosci. Lett. 254, 137–140.

Ueda, N., Yamanaka, K., Yamamoto, S., 2001. Purification and characterization of an acid–amidase selective for *N*-palmitoylethanolamine, a putative endogenous anti-inflammatory substance. J. Biol. Chem. 276, 35552–35557.

Wilson, R.I., Nicoll, R.A., 2001. Endogenous cannabinoids mediate retrograde signalling at hippocampal synapses. Nature 410, 588–592.